Geochemistry and tectonics of the Formation of SahandDacitic Dome, Southeast of Tabriz (Northwest of Iran)

Farhad Pirmohammadi Alishah

Department of Geology, Shabestar Branch, Islamic Azad University, Shabestar, Iran.
* Corresponding Author: Petrofarhad@iaushab.ac.ir

Abstract

Sahand volcanic-sub-volcanic Dome, along with several other magmatic domes in northwest Iran and the southern part of Tabriz Fault show adakitic geochemical characteristics. Sahand Dome has mainly dacitic composition. The SiO_2 content and Mg number of Sahand Dome range from 64 to 73 wt% and 27 to 57 respectively. Sahand Dome can be classified as High Silica Adakitic (HSA) type. The rocks studied have porphyritic texture and phenocrysts with plagioclase, sanidine, amphibole, biotite and quartz. Based on geochemical data and multi elements pattern, these rocks are medium to high K calc-alkaline suite and show LILE and LREE enriched normalized multi-element patterns, and Nb and Ti deplated. Chondrite normalized REE patterns of the studied volcanic rocks display a decrease from LREE to HREE without any Eu anomaly and formed in subduction zone in an active continental margin. The geochemical characteristics of Dome demonstrate that it has been formed in a post-collision setting. Given the generative model and the formation environment of these rocks, the upper Miocene age of Sahand Dome and middle Miocene closure age of Neo-Tethys, the genesis of these rocks can be associated with Neo-Tethys geodynamic processes, in a way that with complete closure of Neo-Tethys in the middle to upper Miocene, the collision of Arabian plate with Iranian central plate caused crustal thickening at the collision zone in the early upper Miocene. Post-collision stretching forces caused stretching of lithosphere and delimination of the lower crust at the collision zone. Partial melting of deliminated lower crust and its relative contamination with mantle materials caused the formation of Sahand Dacitic Dome.
Keywords: Sahand, Adakite, Dacite, Partial melting, Neo-Tethys.

1- Introduction

The latest geological studies on volcanic rocks of Iran,indicate that there is evidence, for existence of rocks with adakitic nature (Jahangiri, 2007). Adakites have an intermediate to acidic composition and are identified with high ratios of Sr/Y and La/Yb (n) (Wang et al. 2006). Discovering such rocks in Iran necessitated more detailed studies on the origin and tectonic setting of volcanic rocks which is helpful to find the reason of magmatism, the differences between them and the forming of rocks with different nature (Jahangiri, 2007).

The subduction of Neo-Tethys beneath the Iranian Central Block caused extensive magmatic activity in Orumieh-Dokhtar magmatic belt in Iran (Shahabpour, 2005). The NW–SE-trending UrumiehDokhtar magmatic assemblage, is oriented parallel to the Zagros Thrust (Fig. 1). The peak of magmatic activity in this belt occurred in Eocene, but continued until Quaternary with a short break. The main magmatic activities formed volcanic rocks, which it was accompanied by magmatic intrusions at specific time intervals. Geochemical characteristics of the rocks of this belt show subduction setting signature

(Shahabpour, 2005). Omrani et al. (2008) study on the central and southeastern parts of the belt, show calc-alkaline nature for Paleogene rocks and adakitic nature for Neogene/Quaternary rocks.

Jahangiri (2007) researches on some samples of Sahand (the studied Dome in this paper) and other domes in South Tabriz Fault indicate an adakitic nature for them which have formed in the later stages of the collision.is one of those studies carried out in the study area of northwest Iran. He among others studied and considered developed. In this paper, we provide an overview on geology of Sahand volcanic dome and present more whole rock analysis to constrain the petrogenesis and geodynamic setting of the Dom.
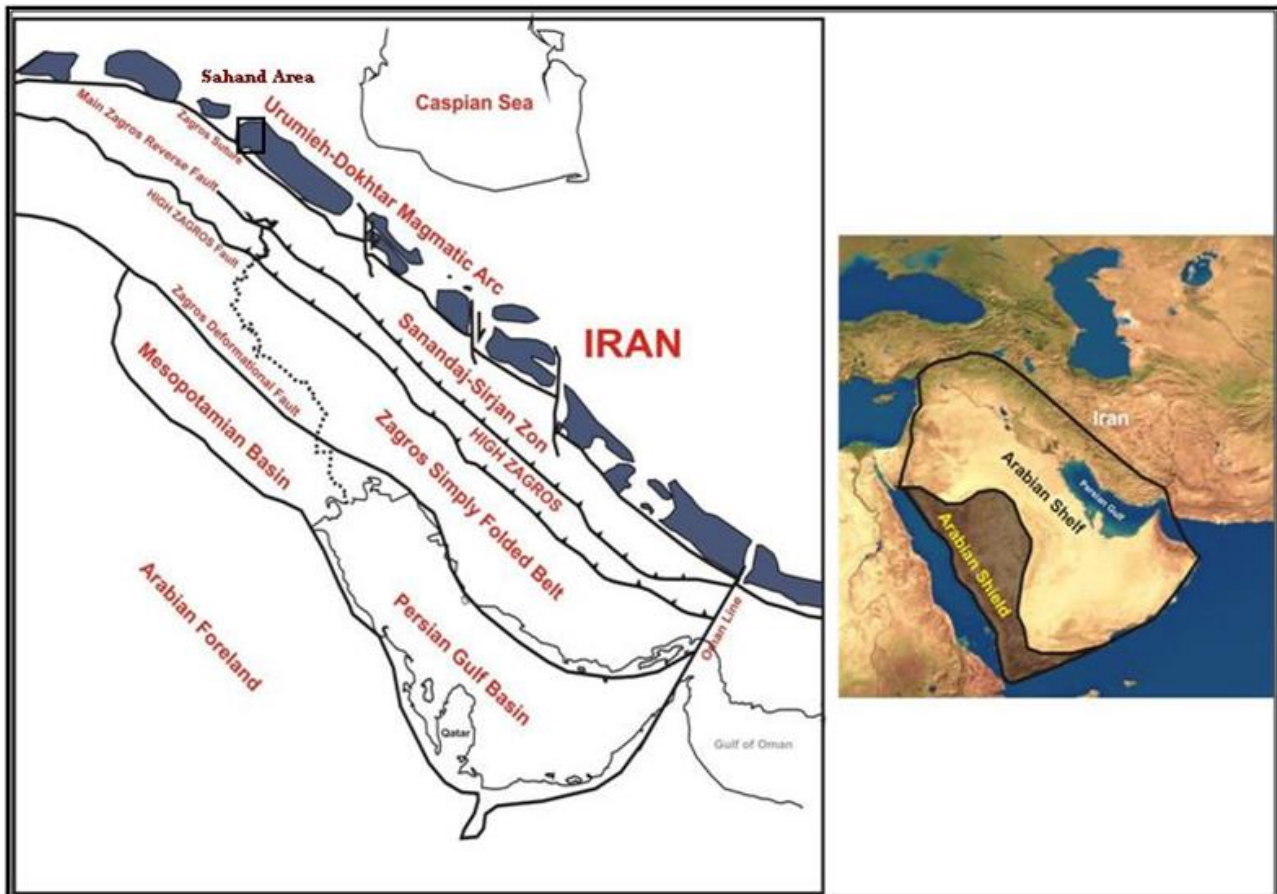

Figure 1) Three main tectonic units of the Zagros orogenic belt. Thestudied area outlined by the box (Map from Allen et al., 2004).

2- Regional Geology

Volcanic to sub-volcanic Sahand Dome is located in southeast of Tabriz and south of Tabriz Fault in northwest Iran (Fig. 2). Sahand Dome is one of several (about 30) sub-volcanic domes of the south of Tabriz Fault trending northwest–southeast. The dome mainly is composed of dacite and minor component is rhyodacite, with porphyritic texture with large plagioclase, biotite and hornblende crystals, (Fig. 3). They are not perfectly round and identifiable in most of the regions around the dome, in a manner that the rocks belonging to the dome have been infiltrated in a flood-like form into the rocks surrounding the dome. An outcrop of arched like of Sahand rocks is observed in the southwestern of it within the older units. The rocks of these arched like have graolar to porphyritic texture whit aphyric matrix. Sahand dome belongs to the magmatic zones of Urmia-Dokhtar or Azerbaijan-Alborz (Fig. 1) which was resulted from the Neotethys subduction. Miocene basal conglomerate has been located on the top of one of the domes

indicates that these domes have been formed before Miocene. Due to the absence of fossils in these units, their exact age is unknown. Jahangiri (2007) called them Miocene units (Upper Red Formation). However, no age-dating data has been reported for these domes yet. So the evidence shows that these domes are older than the Miocene (Jahangiri, 2007).
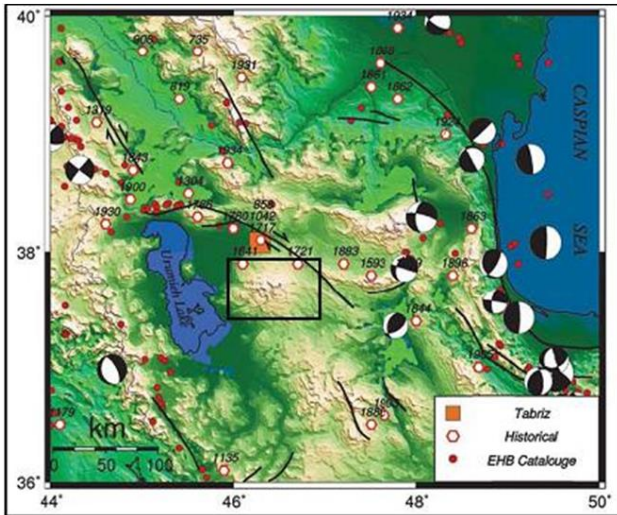

Figure 2) Tectonic map of the studied area that show by a square, studied area bounded by Tabriz fault and Urumieh Lake (Ambraseys and Melville, 1982).
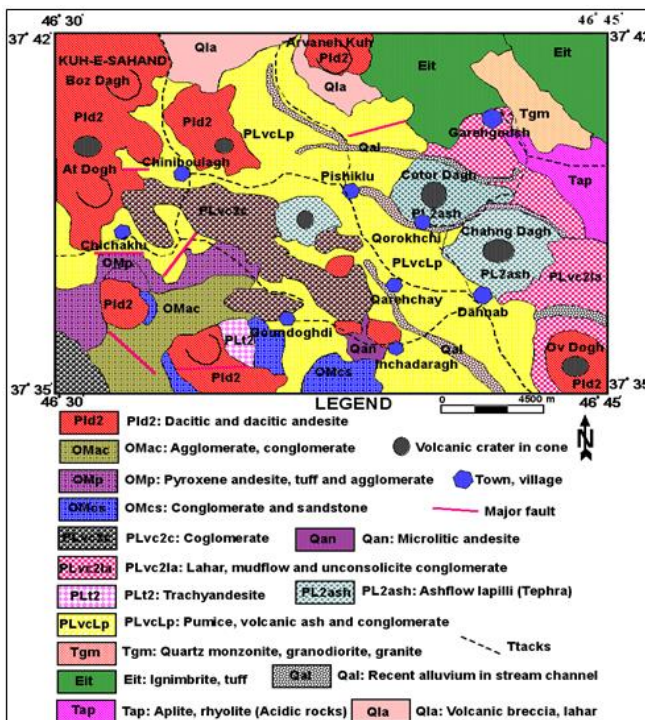

Figure 3) Geological map of the study area, adapted from the 1:100000 geological map of Bostanabad (Behrouzi et al., 1997).

Based on the description of the geological map of Bostaabad region (Fig. 3), stratigraphy of the region can be explained as follows: The oldest geological units of the Cambrian exist in the area around Sahand Dome. These units have been formed by dolomite and altered mica-bearing shale belonging to Zaigun and Lalun formations. Shale, sandstone, and limestone are Devonian units which, along with Permian sediments. Permian sediments in this region are mainly composed of gray limestone, which are converted to shale at the top section. Gray dolomites, vermicular limestone and lime shale (Elika Formation) form the Triassic sediments covered by the Eocene units.

3- Analytical Method

In order to correctly characterize their chemical composition, 30 samples were chosen for major, trace and rare-earth element (REE) analysis. Samples for whole rock analysis were crushed and powdered in agate ball-mills. Major elements were determined by ME-ICP method. Inductively Coupled Plasma-Mass Spectrometry (ICP-MS) was employed for REE and trace element analysis for all of the samples. All of the analyses were determined at Actlabs Laboratories (Canada) (Pirmohammadi Alishah, 2011).

4- Petrography

Field and microscopic studies on volcanic rocks of Sahand Dome show that they are composed of dacite and rhyodacite. Geological and petrological descriptions for each rock unit are given below.

Dacite - riodacite: They have a porphyritic texture with phenocrysts of plagioclase, quartz, hornblende and biotite. In some cases they show glomeroporphyritic texture. Phenocrysts vary in size from 2 to 5 mm mafic rocks xenoliths can be seen within the rocks (Fig. 4a). Anhedral quartz with embayed margins is as phenocrysts

and inclusions in biotite, plagioclase, and orthose (Fig. 4b). They are also of they are characterized by 25-40% plagioclase phenocryst with disequilibrium evidence of magma They show zoning, polysynthetic and carlsbad twiings and inclusions of apatite, opaque, amphibole and zircon (Fig. 4c). Hornblende as another phenocryst of some dacites have concentration less than plagioclase It is altered to epidote, sericitic and chlorite. Biotites have inclusions of quartz or other minerals. In some cases, These rocks are composed of very fine groundmass conform of plagioclase, alkali feldspar, and quartz crystals. Apatite and zircon of accessory minerals of these rocks which are found as inclusions in phenocrysts or in the basis (texture) of these rocks.
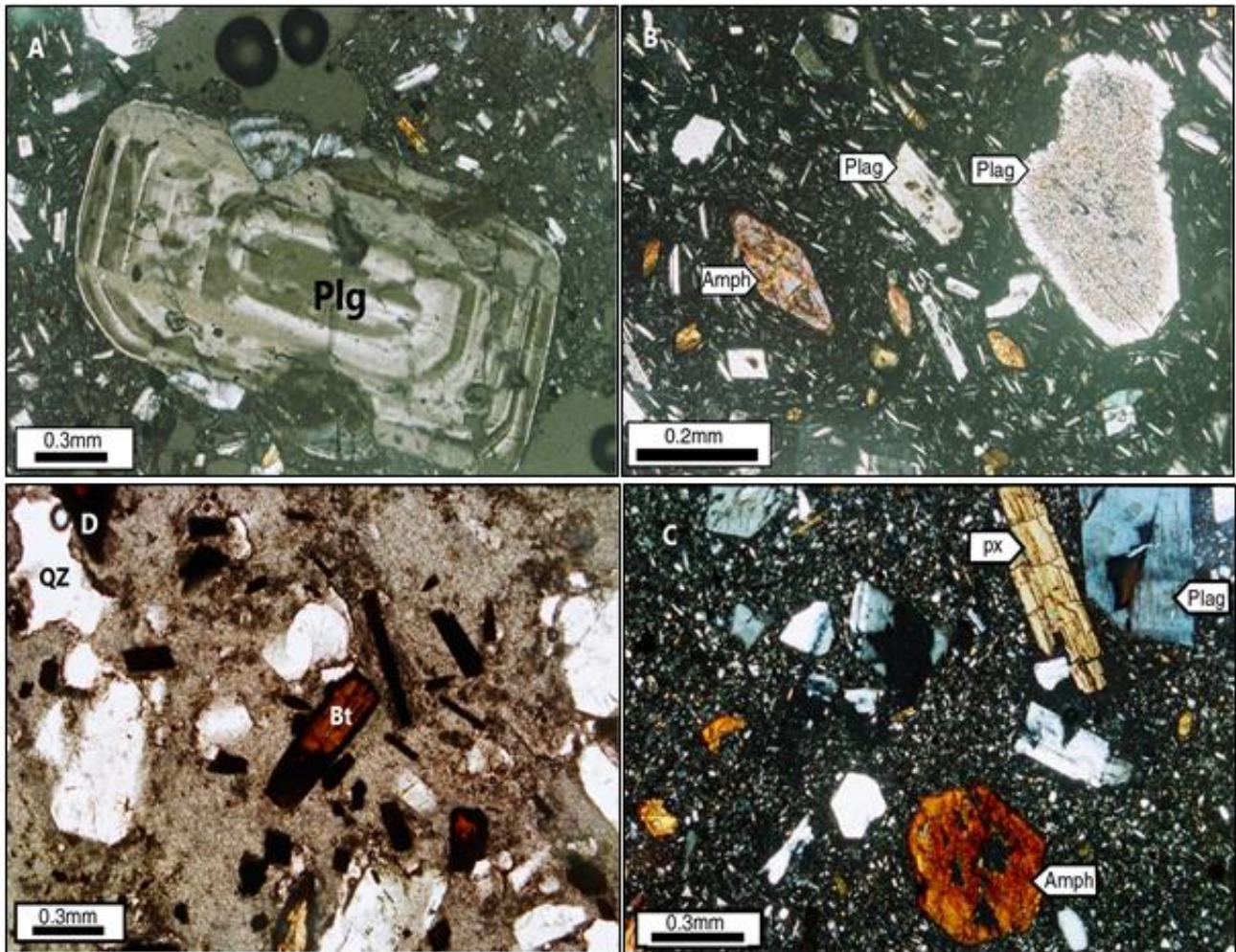

Figure 4) Pictures from the rock collection of Kiamaki Dome in the desert and under microscope, for more details see the text.

Andesite: This group of rocks is usually darker than dacites in color. In these rocks, phenocrysts are composed of plagioclase, hornblende, and biotite. Phenocrysts in which mainly have formed glomeroporphyritic texture. These rocks, have a porphyritic texture and fine-grained groundmass. The grundmass are mainly composed of plagioclase, hornblende, quartz, apatite (less than 5 percent) and pyroxene. Plagioclase is the main and most abundant phenocryst in these rocks, which is seen as euhedral to subhedral. They have polysynthetic, Carlsbad and zoning in some samples (Fig. 4d). Their amount changes in a range of 15 to 40% of the total volume of the rock. Some plagioclases have oxidized margins; that is, they have become opaque. Amphibole phenocrysts are the most abundant phenocrysts after plagioclases, which has been opacitized. Microlites are often composed of plagioclases. Alkali feldspar, quartz, pyroxene, opaque

minerals, carbonate and apatite are found in very small scale in the rock groundmass.

5- Whole rock geochemistry and geological setting

In the classification diagrams of SiO_2 versus K_2O adopted from Le Maitre (2002) and SiO_2 versus Zr/TiO_2, the Sahand dome samples plot in the field of dacite and rhyodacite which show sub-alkaline affinity (Fig. 5). In the Harker diagrams, (Fig. 6), they have negative trend in Fe_2O_3, MgO, TiO_2, CaO, Zn, Sr, Ti and Y versus SiO2, represent the fractionation of

apatite, hornblende and plagioclase from magma. Decreases of SiO_2 and La with an increased value of Al_2O_3 and increasing of Sr/Y with SiO_2 content indicate crystal segregation under high pressure (Karsli et al., 2010). In Harker diagrams, volcanic and intrusive rocks of Sahand Dome have been distributed in a linear trend which indicates an equal source for them. Amounts of Na_2O, K_2O versus SiO_2 show a scattered trend that could be the result of assimilation and fractional crystallization which is confirmed by the presence of different lithospheric xenoliths in the rocks of this Dome.
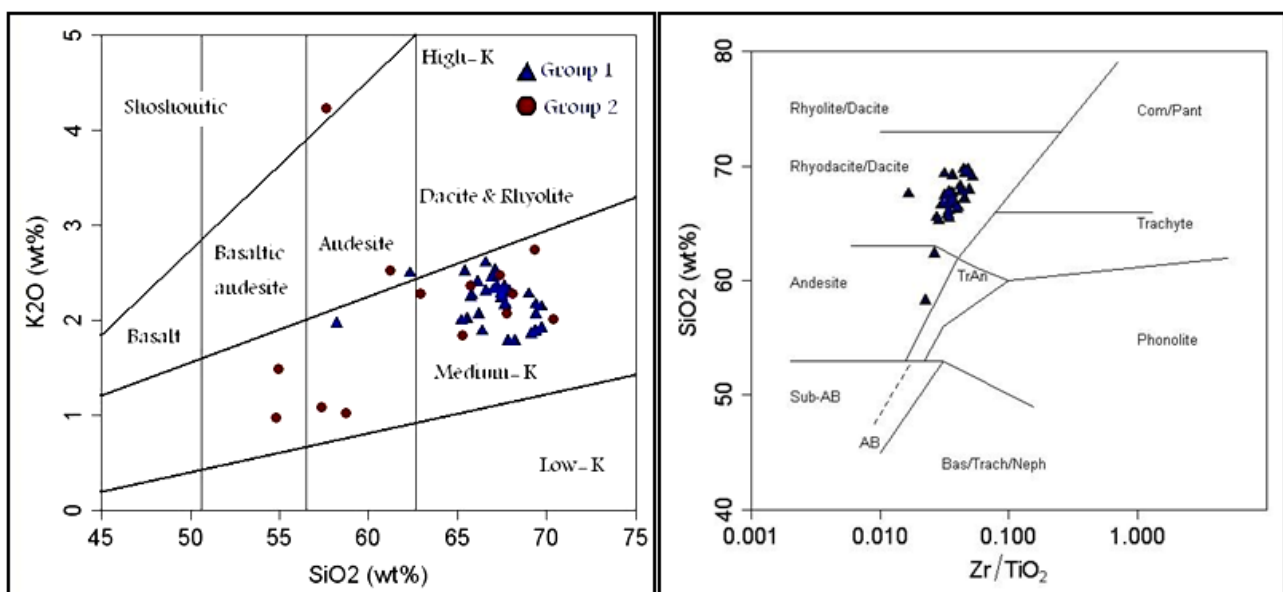

Figure 5) Diagram ofSiO₂ versus K₂O adopted from Le Maitre (2002) and Zr/TiO₂ versus SiO₂, adopted from Winchester and Floyd (1977).

The chondrite normalized Rare Earth Element (REE) patterns of these rocks (Fig. 7). They show depletion in HREE with a flat trend. In multi-element pattern normalized to the primitive mantle (Fig. 7) samples show enrichment in LILE such as Pb, U, Cs, K, and Sr and depletion in Nb.

These rocks have low concentration of HREE and Y (8.1-3.9ppm). Considering these characteristics, along with high levels of Sr and high ratio of Sr/Y, these rocks can be classified in the diagram of Y versus Sr/Y as adakites (Fig. 8a). In the diagram of La/Sm (n) versus Nb/Th adopted from Wang et al. (2006) the studied rocks are located in the adakites' area (Fig. 8b).

Geochemical characteristics of the studied samples such as the concentration of Th and ratios of Th/Sm, Th/Yb and Th/Ce show that these rocks are in a post-collision position (Figs. 9a and b).

6- Discussion

6.1- Origin characteristics

In continental subduction zones, magma can be the result of two main origins: the upper crust and lower crust-upper mantle and a composite origin: crust-mantle (mix), caused by fluids of the subducted plate. partial melting of subducted sediments and fluids originated from the subducted slab metasomatize or enrich the

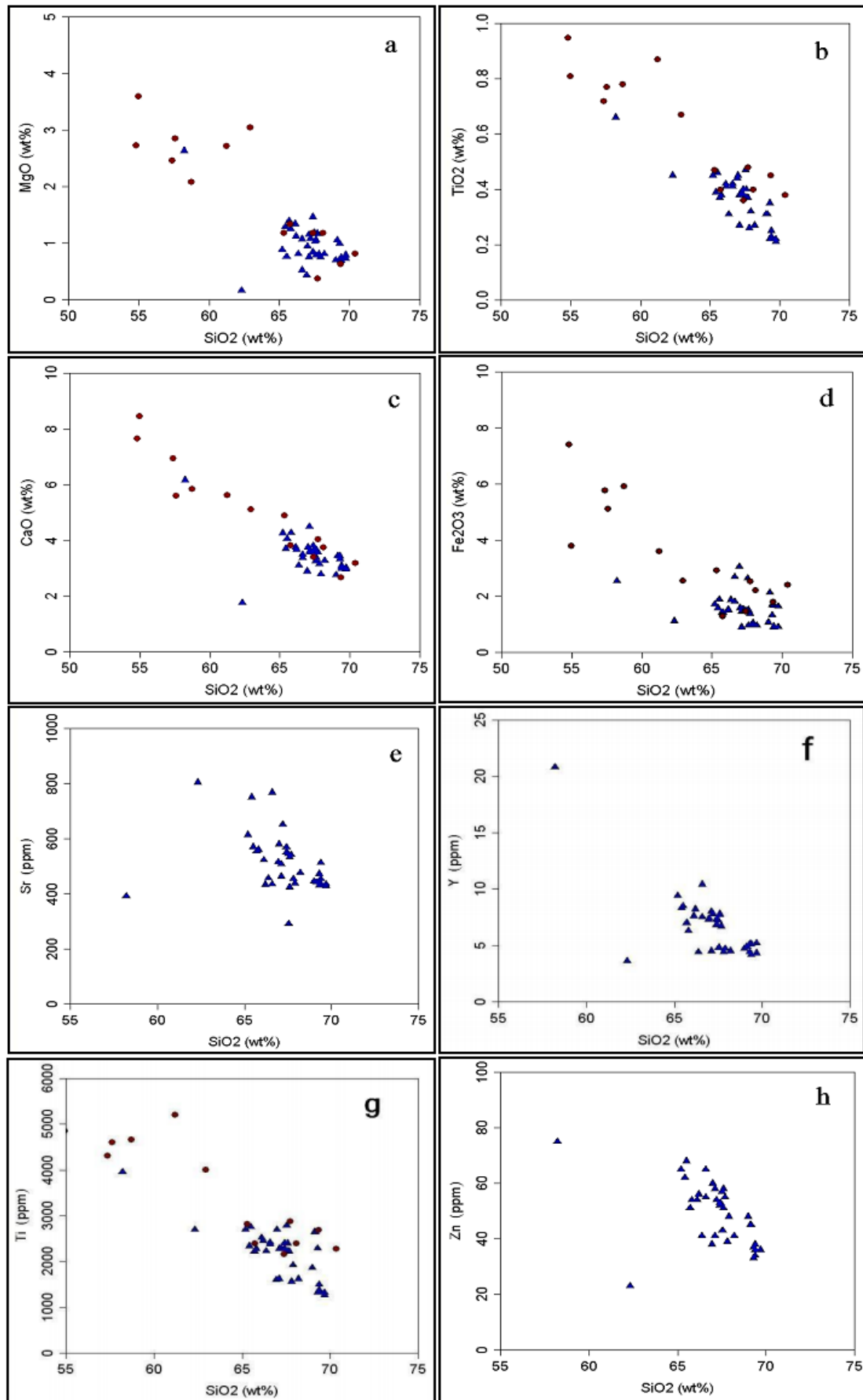origin of magma in subducted zones (Elburg et al. 2002; Guo et al., 2005).

Figure 6) Diagrams of the changes in the various elements versus SiO2 (HPFS crystal fractionation at high pressure by Karsli et al. (2010), symbols are as in Figure 5.
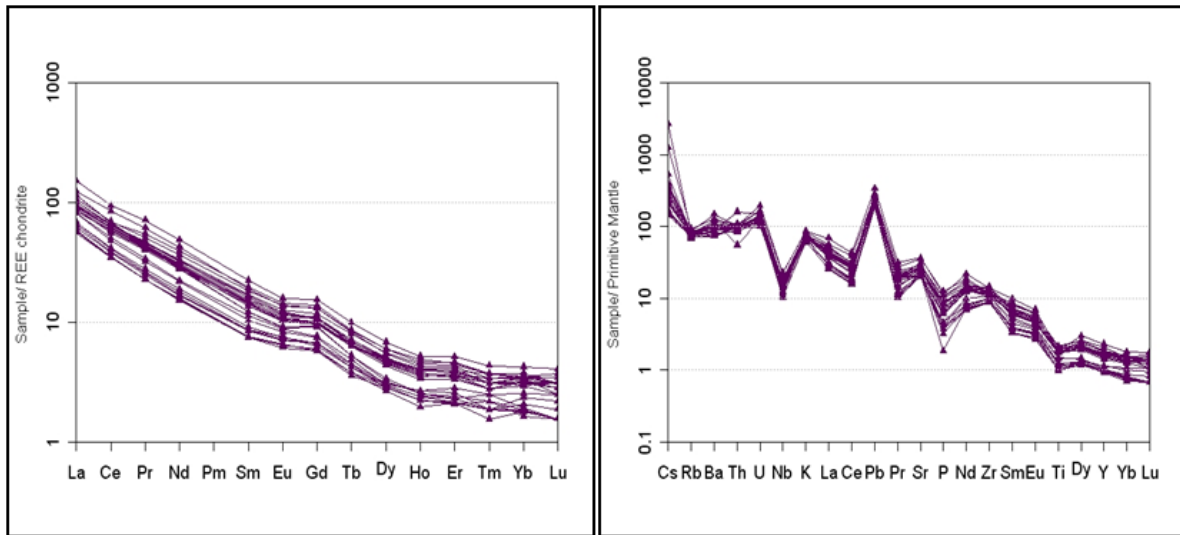
Figure 7. REE diagram normalized to chondrite, Pearce (1983) and multi-element diagram normalized to primitive mantle (Sun and McDonough (1989)) for Sahand samples.
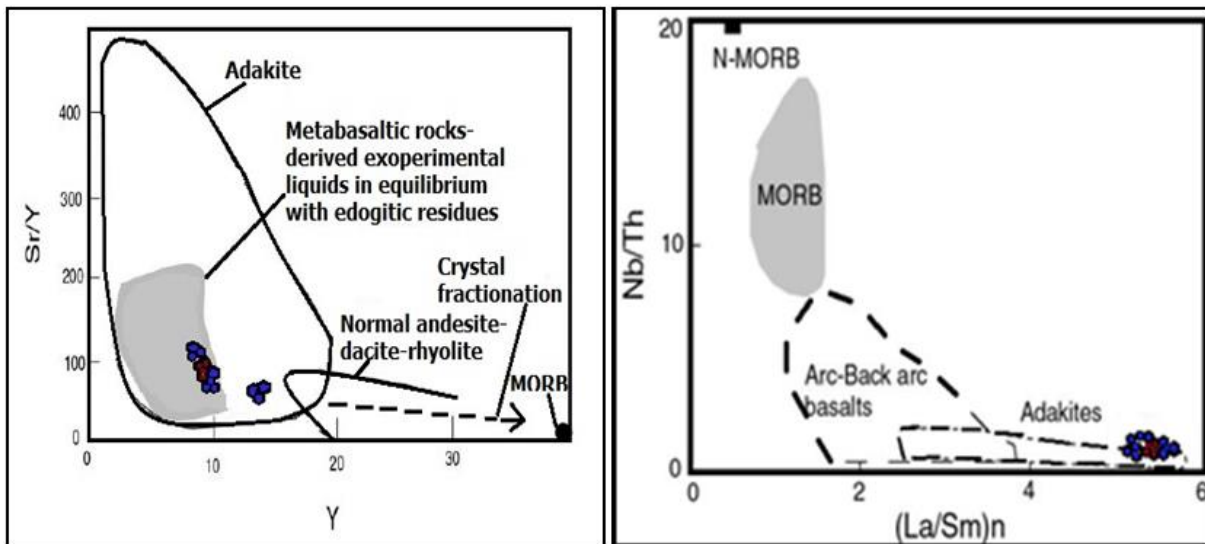

Figure 8a) Plot of Y versus Sr/Y adopted from Petrone et al. (2006). b) diagram La/Sm (n) versus Nb/Th adopted from Wang et al. (2006) for the samples studied, ranges as in Figure 7, Symbols specified as in Figure 5.
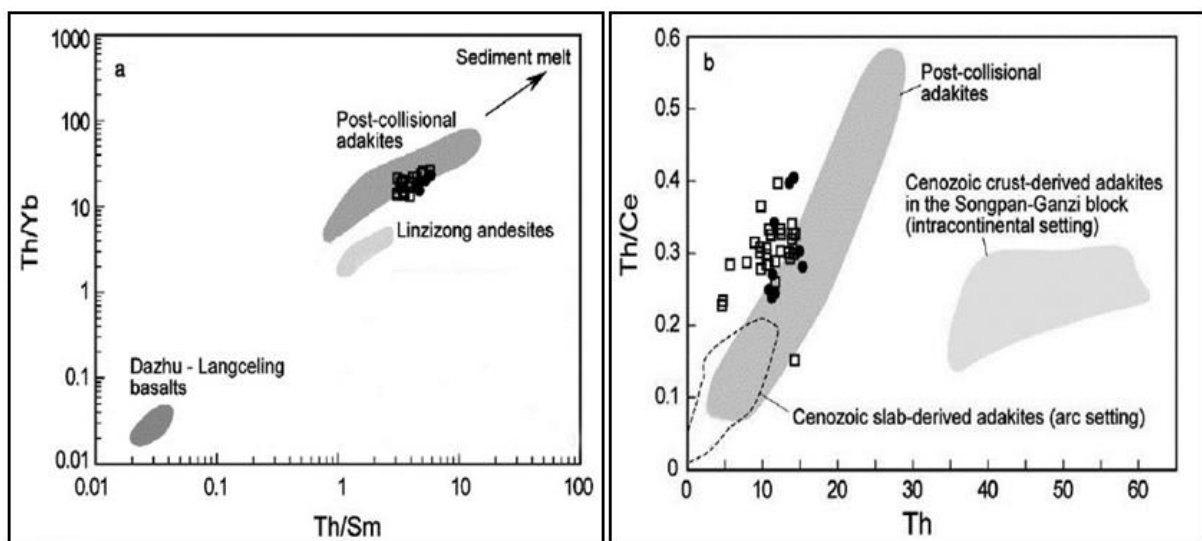

Figure 9. (a) Plot of Th/Sm vs. Th/Yb, (b) Plot of Th vs. Th/Ce adopted from Guo et al., (2005) and Guo et al. (2007).

The high ratio of LREE/HREE Sahand samples can be the result of these processes. The high ratios of Sr/Nd in the samples related to subducted zones are caused by the impact of fluids originating from subducted plate and this could be due to incomplete dissolution also. Instead, the high ratio of Th/Yb and low ratio of Sr/Y represent the effect of subducted sediments melting (Elliot et al., 1997). Sahand samples have Sr/Nd = 22-63 and Th/Yb = 13-26 ratios. These ratios together with the limited fluctuations of Zr/Y ratio (16-22) indicate the greater impact of fluids originating from the subducted slab for the parent magma of Sahand adakite. Depletion in some HFSEs indicates the presence of rutile or amphibole in residue and probably the garnet-amphibolite or amphibole-eclogite source (origin) in these rocks.
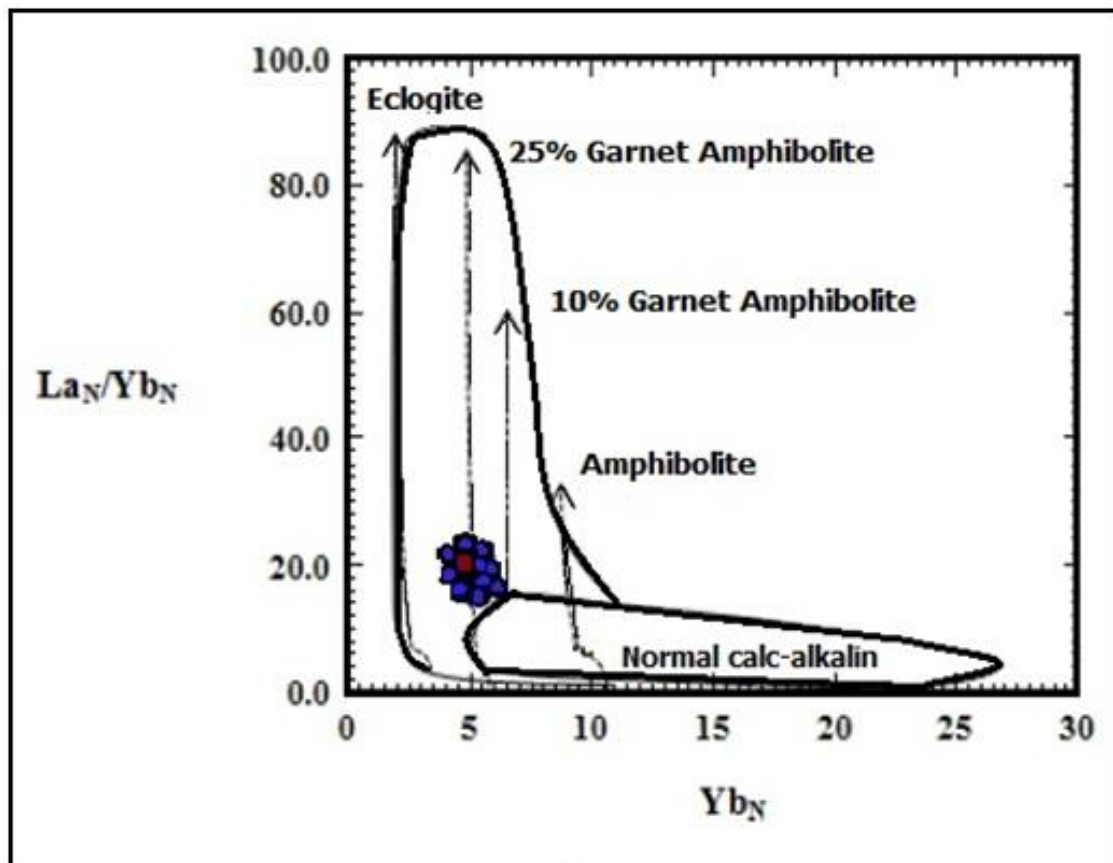

Figure 10) Plot of Yb vs. La/Yb for Sahand samples adopted from Martin (1999) with identified curves adopted from Irving and Frey (1978), Fujimaki et al. (1984), Sisson (1994). Symbols are as in Figure 5.

The enrichment of Sr and the absence of negative Eu anomalies indicate that the residual source was plagioclase–free. The Nb and Ti are strongly depleted in the studied samples, which suggest that the source also has residual rutile and amphibole and thus was most probably hydrous garnet–amphibolite or eclogite. This garnet–bearing source implies that there are at least two possibilities for generation of adakitic rocks in Sahand: 1) partial melting of thickened lower crust and 2) melting of subducted oceanic slab of the Neotethys. It is expected that crustal thickening caused by the Arabian–Asian continental collision would result in transformation of basaltic lower crust in to garnet–amphibolite or eclogite. However, such deeper crustal materials have not been observed nor reported as xenoliths from the studied area. Moreover, according to the Moho depth map of (Dehghani and Makris, 1984) the crustal thickness of the area ranges from 48 to 50 km. Based on plot La/Yb versus Yb, Sahand samples have been generated by less than 25% partial melting of an amphibolite origin containing 3% garnet (Fig. 10).

6.2- Genetic pattern of Sahand Adakitic Dome

Studies on adakites show five genetic models for them in different environments (Wang et al., 2006):

1- Partial melting of subducted oceanic plate.
2- The processes of crustal contamination and crystal segregation on source basaltic magma.
3- Partial melting of the slab collapsed in the mantle.
4- Partial melting of mafic rocks in the lower part of the thickened crust.
5- Partial melting of the lower and laminated (deliminated) crust.

Geochemical characteristics of these rocks suggest the very minor effect of ACF process on their genesis. Th and Th/Ce ratios in the studied samples are higher than the values of these elements in the dacites derived by partial melting of subducted oceanic crust (Fig. 11). The contrast between felsic melts generated from the partial melting of subducted oceanic plate and mantle wedge causes decreased SiO2 and Na_2O ratios and increased Sr, Mg, Ni, and Cr ratios in the melting phase. This causes a positive relationship of Al_2O3 with SiO_2, and a negative relationship of Na_2O and K_2O with SiO_2.

These geochemical characteristics are common in most adakits (Kay et al., 1993; Rapp et al., 1999), while the Sahand samples do not show these geochemical parameters (Fig. 6). This may indicate no simultaneous involvement of partial melting of the subducted oceanic plate and mantle wedge in the genesis of these rocks.

The MgO values of the studied samples (0.38-2.29 wt%) were less than the MgO in melts originating from the subducted oceanic crust (MORB = 8 wt%, Rapp et al., 1991). These reasons can reject the generative model of Sahand adakites based on the first three models.
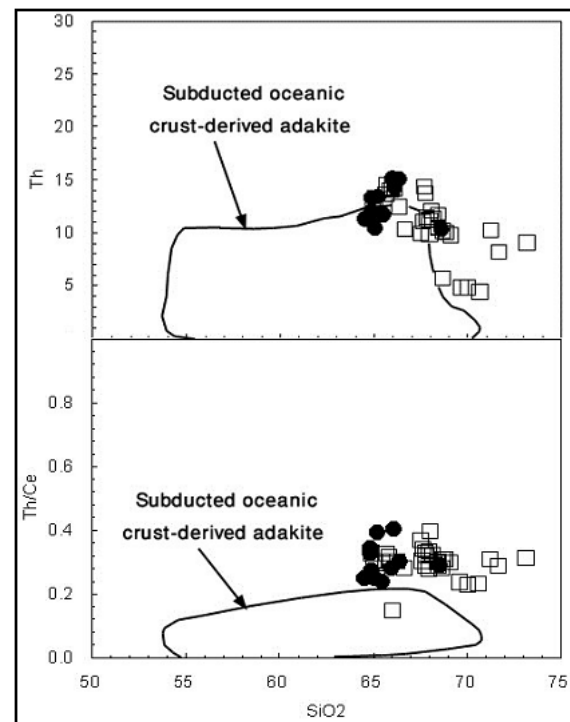
Figure 11) Plots of SiO_2 vs. Th and Th/Ce, their specified limits adopted from Wang et al. (2008). Symbols are as in Figure 9.

Figure 12) REE and multi-element patterns with the areas specified for different adakites adopted from Wang et al., 2008. The area of Sahand adakites has been marked in red. Diagram (a) has been normalized to Boynton (1984) and diagram (b) has been normalized to Sun and McDonough (1989).

The geochemical characteristics of the studied rocks were significantly different from the geochemistry of rocks obtained using the third

model. In the values of La/Sm (n) and ratios of Nb/Th, given in the form of diagrams in Figure 8b, the geochemical differences are well-illustrated.
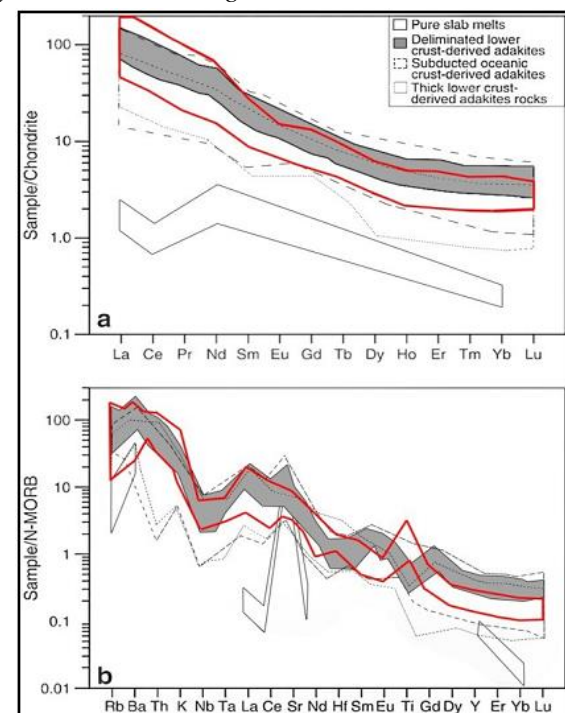
Geochemical show the similarities beetwen Sahand samples and adakites obtained by these two models. REE and multi-element patterns of Sahand samples are similar to the pattern of thickened or deliminated lower continental crust–derived adakites. In the studied samples, Ba show more enrichment than Rb and Th and they have relatively high Nb/Ta ratio (between 12.2 and 19.2). This feature is similar to the thickened or deliminated lower continental crust-derived adakites (Xiong et al., 2003, Xu et al., 2002), but is different from adakites derived by the subducted slab melting (Kay et al., 1993, Kepzhinskas et al., 1996). Almost all elements except Ti in Sahand adakites show a trend similar to the lower thickened or deliminated crust-derived adakites in the multi-element and rare earth element spider diagrams of normalized standard samples (Fig. 12).

4- Conclusions

Sahand Dome is located in the northwest region of Urmia-Dokhtar zone. Relatively studies have shown that adakites are rare the active subduction zones and usually they have been found in the young collision or post-collision setting (Sajona et al. 2000, Guo et al. 2007). In Iran, given the closing age of Neo-Tethys (today, it is agreed on lower or middle Miucen as the closing age) and the age of adakitic rocks which are younger than middle Miocene, this theory can be generalized to Iranian adakites (Berberian et al., 1982; Sengör and Natalin, 1996; Azizi and Moinvazeri, 2010; Mehdipour Ghazi et al., 2012). Jahangiri (2007) attributed the magmatic and adakitic domes in North Tabriz Fault to a post-collision position.

This research shows that the age of Sahand rock is younger than the closing age of Neo-Tethys and collisions. On the other hand, taking into account the horizontal distance from the subduction place of Neo-Tethys (Zagros Fault) and the position of Sahand Dome or Alborz-Azerbaijan zone, the crust thickness increases by continental collision. In general, after each continental collision, an extension condition occurs. Deliminated mafic lower crust is generated due to this post-collision extension phase and causes thickening of the continental crust (Wang et al. 2008). Crust thickening starts from the lower crust, where gabbro converts to eclogite. In this case, this part of the crust becomes denser than mantle lithosphere surrounding this crust. Therefore, this part of the crust is floating within the less dense mantle after being deliminated (low density) (Kay and Kay, 1993).

References:

Allen, M., Jackson, J., and Walker, R., 2004. Late Cenozoic reorganization of the Arabia-Eurasia collision and the comparison of short-term and long-term deformation rates: Tectonics: 23. Doi: 10.1029/2003TC001530.

Ambraseys, N. N., Melville C. 1982. A history of Persian earthquakes, Cambridge University Press.

Ayers J.C., Watson E.B. 1991. Solubility of apatite, monazite, zircon, and rutile in super critical fluids with implications for subduction zone geochemistry", Philosophical Transactions: Physical Sciences and Engineering: 335, 365–375.

Azizi, H., Moinevaziri, H. 2009. Reviewof the tectonic setting of Cretaceous to Quaternary volcanism in northwestern Iran. Journal of Geodynamics: 47, 167–179.

Behrouzi, A. Amini Fazl, A. Amini Azar, B. 1997.Geological Survey of Iran, 1:100,000 Series, Sheet 5265, Bostanabad.

Berberian, F., Muir, I.D., Pankhurst, R.J., Berberian, M. 1982. Late cretaceous and early Miocene Andean type plutonic activity in northern Makran and central Iran. Journal

of Geological Society of London: 139, 605–614.

Boynton, W. V. 1984. Cosmochemistry of the rare earth elements: meteorite studies. In: Henderson, P. (Ed.), Rare Earth Element Geochemistry. Elsevier, Amsterdam, pp. 63–114.

Dehghani, G.A.,Makris, J. 1984. The gravity field and crustal structure of Iran, Neues. Jahrbuch für Geologie and Palaeontologie Abhundlungen: 168, 215–229.

Elburg, M.A., van Bergen, M., Hoogewerff, J., Foden, J., Vroon, P., Zulkarnain, I., Nasution, A. 2002. Geochemical trends across an arc-continent collision zone: magma sources and slab-wedge transfer processes below the Pantar Strait volcanoes, Indonesia. Geochimica et Cosmochimica Acta: 66, 2771–2789.

Elliott, T., Plank, T., Zindler, A., White, W., Bourdon, B. 1997. Element transport from slab to volcanic front at the Mariana arc. Journal of Geophysical Research: 102, 14991–15019.

Fujimaki, H., Tatsumoto, M., Aoki, K., 1984. Partition coefficients of Hf, Zr and REE between phenocrysts and groundmass. Journal of Geophysical Research: 89, 662–672.

Guo, Z., Hertogen, J., Liu, J., Pasteels, P., Boven, A., Punzalan, L., He, H., Luo, X., Guo, Z.F., Wilson, M., Liu, J. Q. 2007. Post-collisional adakites in south Tibet: products of partial melting of subduction-modified lower crust. Lithos: 96, 205–224.

Harker A. 1909. The natural history of igneous rocks, Macmillan, New York, 384pp.

Irving, A.J., Frey, F. A. 1978. Distribution of trace elements between garnet megacrysts and host volcanic liquids of kimberlitic to rhyolitic composition. Geochimica et Cosmochimica Acta: 42, 771–787.

Jahangiri, A. 2007. Post-collisional Miocene adakitic volcanism in NW Iran: Geochemical and geodynamic implications. Journal of Asian Earth Sciences: 30, 433–447.

Kepezhinskas, P., Defant, M. J., Drummond,M. S.1996. Progressive enrichment of island arc mantle by melt-peridotite interaction inferred from Kamchatka xenolithsGeochimica et Cosmochimica Acta: 60,1217–1229.

Karsli, O., Dokuz, A., Uysal, I., Aydin, F., Kandemir, R., Wijbrans, J.2010. Generation of the Early Cenozoic adakitic volcanism by partial melting of mafic lower crust, Eastern Turkey: Implications for crustal thickening to delamination, Lithos: 114, 109–120.

Kay, R.W., Kay, S.M., 1993. Delamination and delamination magmatism. Tectonophysics: 219, 177–189.

Le Maitre, R.W., Streckeisen, A., Zanettin, B., Le Bas, M.J., Bonin, B., Bateman, P., Bellieni, G., Dudek, A., Efremova, S., Keller, J., Lamere, J., Sabine, P. A., Schmid, R., Sorensen, H., Woolley, A. R. 2002. Igneous Rocks: A Classification and Glossary of Terms, Recommendations of the International Union of Geological Sciences, Subcommission of the Systematics of Igneous Rocks. Cambridge University Press, ISBN 0-521-66215-X.

Martin, H. 1999. The adakitic magmas: modern analogues of Archaean granitoids. Lithos: 46, , 411–429.

Mehdipour Ghazi, J. M., Moazzen, M., Rahgoshay, M., Moghadam, H. S., 2012. Geochemical characteristics of basaltic rocks from the Nain ophiolite (Central Iran); constraints on mantle wedge source evolution in an oceanic back arc basin and a geodynamical model. Tectonophysics 574–575, 92–104.

Omrani, J., Agard, P., Whitechurch, H., Benoit, M., Prouteau, G., Jolivet, L. 2008. Arcmagmatism and subduction history

beneath the Zagros Mountains, Iran: a new report of adakites and geodynamic consequences. Lithos: 106, 380–398.

Peacock, S. M., Rushmer, T., Thompson, A. B. 1994. Partial melting of subducting oceanic crust. Earth and Planetary Science Letters 121,224–227.

Pearce J. A. 1983. The role of sub- continental lithosphere magma genesis at destruction plate margin".In: Hawkesworth, C.J. and Norry, M.J. eds. Continental basalts and mantle xenoliths, Nantwich, Cheshire: Shiva Publications, pp. 230–249.

Pearce, J. A., Norry, M. 1979. Petrogenetic implications of Ti, Zr, Y and Nb variations in volcanic rocks. Contributions to Mineralogy and Petrology: 69, 33–47.

Pearce, J.A., Peate, D. W. 1995. Tectonic implications of the composition of volcanic arc magmas. Annual Review of Earth and Planetary Sciences: 23, 251–285.

Petrone, C. M., Francalanci, L., Ferrari, L., Schaaf, P., Conticelli, S. 2006. The San Pedro–Cerro Grande Volcanic Complex (Nayarit, Mexico): inferences on volcanology and magma evolution", In: Siebe C, Aguirre-Dı`az G, Macı`as JL (eds) Neogene- Quaternary continental margin volcanism: a perspective from Mexico. Geol Soc Am Sp Paper, 402(03), 65–98.

Pirmohammadi Alishah, F. 2011. Geochemistry of adakitic composition of Sahand volcano at the south of Tabriz. 30[th]symposium of Erath Sciences, Geological Survey of Iran, Tehran.

Pirmohammadi Alishah, F. 2011. Petrology, Geochemistry and Petrogenesis of Volcanic Rocks in the East and Southeast of Sahand Volcano with Special Reference to the Pyroclastic Rocks, Ph. D thesis, University of Tabriz, Iran, 198pp.

Rapp, R. P., Shimizu, N., Norman, M. D., Applegate, G. S. 1999. Reaction between slab-derived melts and peridotite in the mantle wedge: experimental constraints at 3.8 GPa. Chemical Geology: 160, 335–356.

Rapp, R. P., Watson, E. B., Miller, C. F. 1991. Partial melting of amphibolite/eclogite and the origin of Archaean trondhjemites and tonalities. Precambrian Research: 51, 1–25.

Rapp, R.P., Watson, E.B., 1995. Dehydration melting of metabasalt at 8–32 kbar: implications for continental growth and crust–mantle recyling. Journal of Petrology: 36, 891–931.

Sajona, F.G., Maury, R. C., Publlier, M., Letirrier, J., Bellon, H., Cotton, J. 2000. Magmatic source enrichment by slab-derived melts in a young post-collision setting, Central Mindanao (Philippines). Lithos: 54, 173–206.

Sengor, A. M. C., Natalin, B. A. 1996. Paleotectonic of Asia: fragments of a synthesis. In Yin, A., Harrison, T. M., (Eds.), The Tectonic Evolution of Asia Combridge University Press, Cambridge, 486–640.

Shahabpour, J., 2005. Tectonic evolution of the orogenic belt in the region located between Kerman and Neyriz. Journal of Asian Earth Sciences: 24, 405–417.

Sisson, T.W. 1994. Hornblende–melt trace-element partitioning measured by ion microprobe. Chemical Geology: 117, 331–344.

Sun, S.S., Mc Donough, W.F. 1989. Chemical and isotopic systematics of oceanic basalts: implications for mantle composition and processes", In: Saunders, AD. And Norry, M.J. (eds), Magmatism in oceanic basins. Geol. Soc. London. Spec. Pub, 42, 313–345.

Wang, Q., Wyman, D.A., Xu, J.F., Wan, Y.S., Li, C.F., Zi, F., Jiang, Z.Q., Qiu, H.N., Chu, Z.Y., Zhao, Z.H., Dong, Y.H., 2008. Triassic Nb-enriched basalts, magnesian andesites, and adakites of the Qiangtang terrane (Central Tibet): evidence for metasomatism by slab-derived melts in the mantle wedge.

Contributions to Mineralogy and Petrology: 155, 473–490.

Wang. Q. Xu.J, Jian. P, Bao.Z, Zhao. Z, Li. C., Xiong. X, Ma. 2006. Petrogenesis of Adakitic Porphyries in an Extensional Tectonic Setting, Dexing, South China: Implications for the Genesis of Porphyry Copper Mineralization. Jouranl of Petrology: 47, 119–144.

Winchester J.A., Floyd P.A. 1977. Geochemical discrimination of different magma series and their differentiation products using immobile elements". Chemical Geology: 20, 325–343.

Xiong, X.L., Li, X.H., Xu, J.F., Li, W.X., Zhao, Z. H., Wang, Q. 2003. Extremely high-Na adakite-like magmas derived from alkali-rich basaltic underplate: the late Cretaceous Zhantang andesites in the Huichang Basin, SE China. Geochemical Journal: 37, 233–252.

Xu, J.F., Shinjio, R., Defant, M.J., Wang, Q., Rapp, R. P. 2002. Origin of Mesozoic adakitic intrusive rocks in the Ningzhen area of east China: partial melting or delaminated lower continental crust? Geology: 12, 1111–1114.